Smith Predictor Based Control in Teleoperated Image-guided Beating-heart Surgery

Meaghan Bowthorpe, Mahdi Tavakoli, PhD, and Harald Becher, MD, PhD, FRCP, Robert Howe, PhD

***Abstract*— Surgery on a freely beating-heart is extremely difficult as the surgeon must perform the surgical task while following the heart's fast motion. However, by controlling a *teleoperated* robot to continuously follow the heart's motion, the surgeon can operate on a seemingly stationary heart. The heart's motion is calculated from ultrasound images and thus involves a non-negligible delay estimated to be 100 ms that, if not compensated for, can cause the robot end-effector (i.e., the surgical tool) to collide with and puncture the heart. This research proposes the use of a Smith Predictor to compensate for this time delay. The results suggest that heart motion tracking is improved as the introduction of a Smith Predictor decreased the mean absolute error, difference between the surgeon's motion and the distance between the heart and surgical tool, and mean integrated square error.**

I. Introduction

Beating-heart surgery is a super-human procedure as it requires the surgeon to manually compensate for the heart's fast motion, which has a velocity and an acceleration up to 210 mm/s and 3800 mm/s^2 respectively, while performing a surgical task [1]. Hence, surgical procedures are currently performed on an arrested heart or on a mechanically-stabilized heart [2].

In arrested-heart surgery, a heart-lung machine circulates the blood and ventilates the lungs; however, complications may occur when the heart is restarted. Other side effects include an increased risk of stroke [3] and/or long-term cognitive loss [4]. On the other hand, mechanically-stabilized-heart surgery avoids these dangers but does not eliminate all of the heart's motion. If a teleoperated robot could follow the heart's beating motion, a surgeon could operate on a seemingly stationary heart, completely eliminating these side effects. In addition, normal heart motion during the surgery would allow for *intra-operative* evaluation of a surgical procedure.

This work was supported by the Natural Sciences and Engineering Research Council (NSERC) and by an Alberta Innovates Graduate Student Scholarship awarded to M. Bowthorpe.

M. Bowthorpe is with he Department of Electrical and Computer Engineering, University of Alberta, Edmonton, AB T6G 2R3, Canada (e-mail: meaghan.bowthorpe@ualberta.ca)

M. Tavakoli, PhD, is with the Department of Electrical and Computer Engineering, University of Alberta, Edmonton, AB T6G 2R3, Canada (e-mail: mahdi.tavakoli@ualberta.ca)

H. Becher, MD, PhD, FRCP, is with the Faculty of Medicine and Mazankowski Heart Institute, University of Alberta, Edmonton, AB T6G 2R3, Canada (e-mail: haraldbecher@med.ualberta.ca)

R. D. Howe is with the Harvard School of Engineering and Applied Sciences, Cambridge, MA, 02138 USA, and also with the Harvard Massachusetts Institute of Technology Division of Health Sciences and Technology, Cambridge, MA, 02139 USA (e-mail: howe@seas.harvard.edu)

To develop such a surgical system, the point of interest (POI) on the heart must be tracked in real time. Various sensors such as force sensors measuring the heart's motion through direct contact [5], high-frame-rate video cameras [6], or medical image (mainly ultrasound) scanners [7] can be used to obtain this motion. Medical image guidance was chosen for this study for tracking the POI as this approach can be used for both intracardiac and external procedures. However, acquiring and processing images inevitably introduces a non-negligible time delay. For instance, in a 3D ultrasound scanner, the frame rate can be as low as 18 Hz [8]. The subsequent processing increases the delay, which, if not compensated for, may cause the teleoperated robot end-effector (i.e., the surgical tool) to collide with and puncture the heart.

II. Background

Prior art can be separated into two main categories: *Prediction algorithms*, which *feed-forward* an estimate of the heart's future motion as the reference position for the teleoperated surgical robot controller, and *predictive controllers*, which account for the time delays in a *feedback* structure and are informed by the dynamic characteristics of the surgical robot. Table I categorizes the contributions of past research based on which control method was used, whether medical images were used to obtain the heart's motion, and whether the surgical robot's dynamics were considered.

A. Feedforward compensation of delay through prediction

Most past research involving feedforward compensation of delay through prediction neglects the surgical robot's dynamics and does not include feedback control. A variety of methods for tracking the POI on the heart have been proposed. Yuen et al. compared the performance of three

TABLE I: The previous research has been divided into different categories based on its approach to heart motion tracking and control.

	Prediction or Predictive Control	Image-Based	Robot Dynamics
[1]	Prediction	No	No
[6]	Predictive Control	No	Yes
[9]	Prediction	Yes	No
[10]	Prediction	No	Yes
[11]	Prediction	No	No
[12]	Predictive Control	No	Yes
Proposed Method	Predictive Control	Yes	Yes

heart motion estimators where the heart motion was collected from ultrasound images [9]. These algorithms were designed to control a one-dimensional motion compensating *hand-held* tool for mitral valve repair [1]. The surgical device dynamics did not have to be considered as there was no dynamic effect intervening between the surgeon's hand motion and the rigid tool's motion in a hand-held device. In other words, in a hand-held rigid device, there is no difference between the reference motion commanded by the user who holds the device and the actual motion experienced by the device end-effector. Hence, there is little need for considering the hand-held device dynamics. Clearly, unlike the hand-held device case, device dynamics do matter in a teleoperated device case, which is the focus of this paper. Franke et al. proposed the use of adaptive filters as they are capable of following a slowly varying heart rate [10]. However, the heart's motion was captured with sonomicrometry crystals. Bebek and Cavusoglu employed the electrocardiogram (ECG) to synchronize the beginning of the actual and estimated heartbeats [11]. The heart's motion was once again captured with sonomicrometry crystals that had been sutured onto the heart, which is not practical during surgery.

B. Feedback compensation of delay through predictive control

Predictive controllers use the dynamic model of the robot in a feedback structure to account for the delay inherent in the measurement of heart motion. Ginhoux et al. compensated for the respiratory and the heart beat induced motions separately using a repetitive generalized predictive controller and frequency cancellation respectively [6], [12]. This method did take the robot's dynamics into account, but it did not address time delay compensation as a very high-frame-rate camera (500 Hz) was used to acquire heart motion.

The research reported in this paper builds on the work done by Yuen et al. [9] for controlling a hand-held surgical tool, and takes the next logical step by introducing a predictive control approach that considers *both the time delay due to the image-based heart motion tracking and the teleoperated surgical robot's dynamics in a feedback control structure*. We augment the feedback controller with a modified Smith Predictor to ensure that the teleoperated robot follows the surgeon's hand motion and the heart beat motion despite the time delays caused by medical image acquisition and processing. An estimate of the heart's current motion is added to the system as an additional set point. As well, in the proposed control system, we do consider the difference in the sampling rates between the acquisition of ultrasound images and the surgical robot's update rate.

The remaining sections of this paper are organized as follows. Section III describes a representative application of beating-heart surgery. The research problem is formulated in Section IV. Section V discusses the Smith Predictor and its implementation. Sections VI and VII highlight the simulation

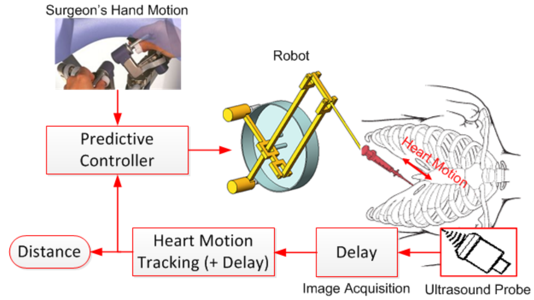

Fig. 1: The teleoperated image-guided beating-heart surgical setup for pericardiocentesis. The needle is inserted through the chest wall and into the pericardial sac to drain excess fluid but it should stop short of the heart tissue [13].

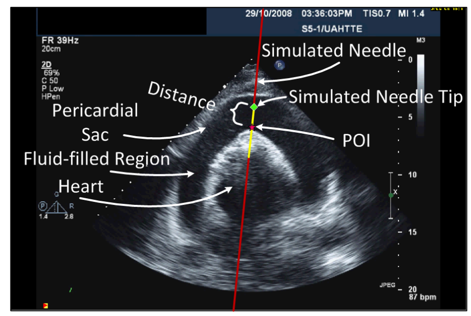

Fig. 2: A 2D ultrasound image from a patient who has a build-up of fluid in the pericardial sac. The red and yellow lines superimposed on the image represent the simulated needle's position. The bright areas of the image are tissue and the dark areas are fluid-filled regions.

and the experimental results respectively. Finally, concluding remarks are presented in Section VIII.

III. A Representative Image-guided Procedure

While the image-based heart motion tracking can be procedure-specific, the Smith Predictor based control method developed in this paper applies to any teleoperated surgery on the beating heart that is performed under medical image guidance.

A. Pericardiocentesis

To begin, a procedure requiring one-dimensional tissue tracking is considered: pericardiocentesis. During pericardiocentesis a needle is inserted into the pericardial sac to drain excess fluid, which is constraining heart function. Currently, ultrasound images are used to find the optimal puncture site but, the needle is inserted with little or no intra-operative image guidance [14]. By using a heart motion-synchronized needle as shown in Fig. 1, the risk of puncturing a coronary artery could be greatly reduced.

B. Image-based tissue tracking

The goal of image-guided robotic assistance is to virtually stabilize the heart. To do so, the distance between the heart tissue and the needle tip is made to follow the surgeon's hand motion. This distance is calculated from ultrasound images using the flashlight method developed by Novotny et al. [15]. Specifically, the axis of the needle, found using a Radon Transform modified for three dimensional data, is extended towards the heart tissue. The POI (the heart wall) is

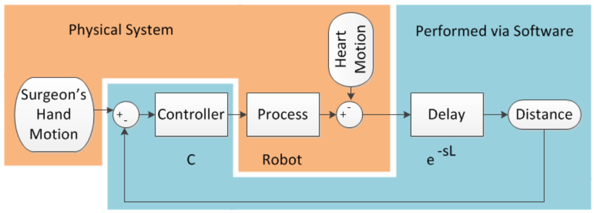

Fig. 3: The initial representation of the feedback controller that controls the robot's motion to follow the surgeon's hand motion.

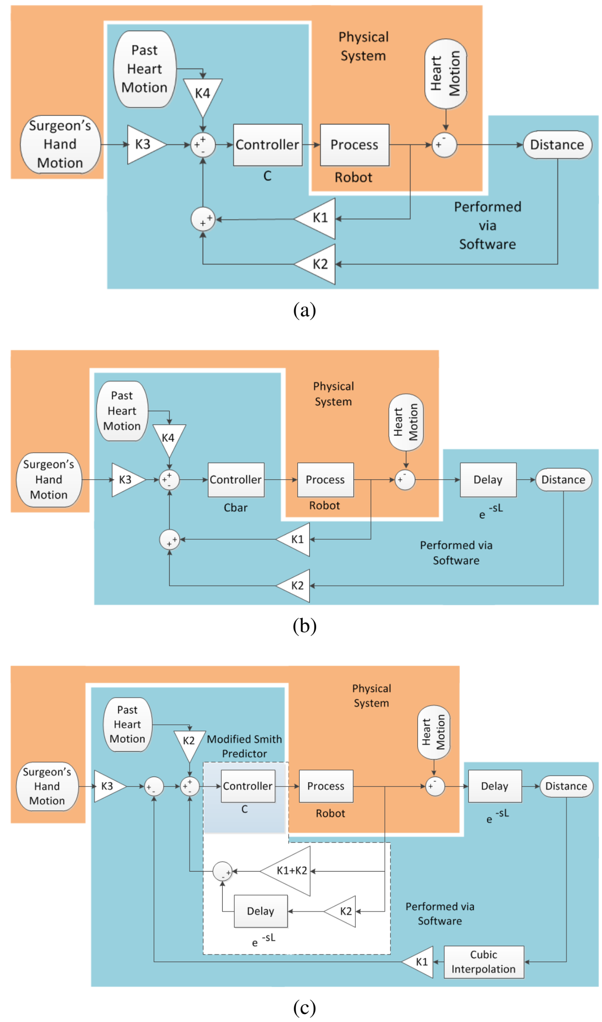

Fig. 4: The feedback controller designed to follow the surgeon's hand motion as well as the heart's motion with the added gain blocks, which increase the number of design parameters, is shown in a). The initial controller is then replaced by a Smith Predictor in b). The complete control loop including the Smith Predictor is shown in c).

the closest change from a dark area (the fluid-filled region) to a light area (the tissue) beyond the needle tip, and is marked by the pink asterisk in Fig. 2. The movement of this tissue location is recorded as the heart's displacement relative to the needle tip.

IV. Problem Formulation

The aim of this research is to virtually stabilize the heart through the use of a teleoperated surgical robot. Because the surgical robot is teleoperated, its dynamics must be taken into account. In addition, the imaging delay must be compensated for while the heart's repetitive motion, as well as the surgeon's hand motions, are followed. A simple feedback control loop representing the unalterable "Physical system", which includes the heart, surgical robot, and surgeon, and the alterable part that is "Performed via Software" is shown in Fig. 3.

To begin, let us make the following observations:

- The heart motion is quasi-periodic,
- The last heart beat's motion can be extracted from the measured distance between the surgical tool and the heart.

Next, we will make the following assumptions:

- The surgical robot is a linear time-invariant system and has one degree of freedom,
- The time delay due to image acquisition/processing is constant and known,

A shortcoming of the system is that the distance data, calculated from the ultrasound images, arrives at a much lower sampling rate than the control update rate of the surgical robot. Thus this slowly sampled data is upsampled to take advantage of the surgical robot's faster operating capabilities. Futhermore, due to the delay present in the feedback loop, the sytem shown in Fig. 3 is unstable and/or has poor performance. To tackle this problem, we use a modified Smith Predictor to compensate for this delay and to ensure that the system remains stable and retains the good performance it would have if the delay could be removed.

V. Proposed Smith Predictor Based Design

A Smith Predictor, first proposed by O. J. Smith in 1957, is a predictive feedback controller that effectively separates the fixed internal delay from the feedback loop [16]. It does not limit one's choice of controller but the length of the constant time delay and the model of the plant must be known. Once the Smith Predictor is implemented, it ensures a control system retains the stability and good performance that it would have if the delay was not present. However, the delayed system will follow the input reference signal in the same manner as the non-delayed system except that the system's response will now be delayed by the length of the system's delay.

A. Controller Design

The configuration of the negative feedback control loop in Fig. 3 only follows the surgeon's hand motion, not the heart's motion. Consequently, an estimate of the heart's motion is added as an another set-point – see Fig. 4a. Since the heart's motion is quasi-periodic, the measured motion from the past heart beat provides an estimate of the heart's trajectory in the current heart beat. An inner loop is added to help the robot follow the heart's (outdated) motion as well as the surgeon's hand (current) motion. In addition, more design parameters in the form of four gain blocks, K1, K2, K3, and K4 have been added: one for each feedback loop, one to scale the surgeon's hand motion, and one to scale the past heart motion. Now, the controller, C, and these gains are calculated based on the no-delay system – Fig. 4a. The transfer function between the three inputs:

R: Surgeon's hand motion

P: Past heart motion

Or: Current heart motion
and the output:

D: Distance between the needle tip and the heart wall is calculated.

$$D = \frac{(K_4CG)P - (1 + CGK_1)Or + (CGK_3)R}{1 + CG(K_1 + K_2)} \tag{1}$$

A proportional controller was chosen for C,

$$C = k. \tag{2}$$

The y-axis 1 joint of the Phantom Premium 1.5A robot, a haptic robot (Sensable group, now part of Geomagic, Wilmington, MA) was chosen as the surgical robot, G [17].

$$G = \frac{s^4 + 30.25s^3 + 2.923 \times 10^5 s^2 + 5.741 \times 10^5 s + 1.784 \times 10^{10}}{1.526s^4 + 233s^3 + 2.848 \times 10^5 s^2} \tag{3}$$

The goal is to make the distance, D, follow the surgeon's hand motion, R. For this reason, the steady-state value of D is calculated when each of the inputs is a step function using the following equation to calculate the gains K_1 to K_4.

$$d(\infty) = \lim_{s \to 0} sD(s) \tag{4}$$

The steady-state value of D is

$$\begin{aligned} &\lim_{s \to 0} s \left(\frac{CG\frac{P}{s} - (1 + CGK_1)\frac{Or}{s} + CGK_3\frac{R}{s}}{1 + CG(K_1 + K_2)} \right) \\ &\approx \frac{P - K_1 Or + K_3 R}{K_1 + K_2}. \end{aligned} \tag{5}$$

The distance, $d(\infty)$, given in (5), must equal the surgeon's hand motion, R_0; therefore the heart's motion, Or_0, and the past heart motion, P_0, must cancel each other. Hence, K_1 must equal 1 as the heart's past motion, P_0, should be approximately equal to the heart's current motion Or_0. Next, for the output to approach R_0, K_3 must be equal to the sum of K_1 and K_2.

The estimate of the heart's motion is based on the past cycle. However, the heart beat can change, so directly shifting the past heart motion will not provide a sufficient estimate. To improve this, an extended Kalman filter (EKF), as described by Yuen et al. [9], is used to calculate the current heart rate. From this rate, the length of time the past heart beat must be delayed to match the current heartbeat is calculated.

Finally, the multi-rate sampling issue is addressed by increasing the slow image acquisition sampling rate to the surgical robot's update rate through the use of a cubic interpolator. The cost of this higher sampling rate is a larger delay, which can be added to the imaging delay and compensated for by the Smith Predictor.

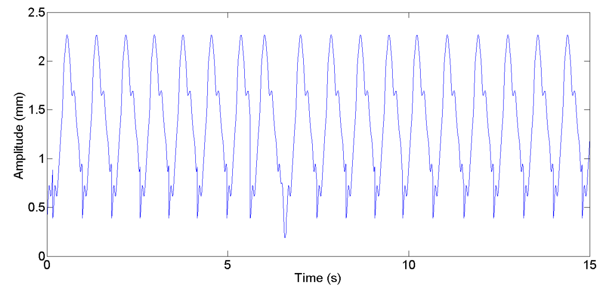

Fig. 5: The averaged distances between the heart wall and the stationary needle tip measured over multiple heart beats from a 2D ultrasound sequence. Each beat has been frequency matched to correspond to an actual clinical heart rate.

B. Smith Predictor Design

Next, the new controller, $\bar{C}$, is designed to preserve the transfer function between the surgeon's hand motion, R, and the distance, D, when the time delay is present – see Fig. 4b. The transfer function between the surgeon's hand motion, R, and the distance, D, becomes

$$D = \frac{\bar{C}GK_3e^{-sL}}{1 + \bar{C}G(K_1 + K_2e^{-sL})}R, \tag{6}$$

where L is the length of the time delay and e^{-sL} represents a constant time delay. By equating the third term of the original transfer function in (1) multiplied by e^{-sL} to (6) and substituting in the values of K_1, K_2, and K_3 found previously, the Smith Predictor $\bar{C}$ is

$$\bar{C} = \frac{C}{1 + CGK_2(1 - e^{-sL})}. \tag{7}$$

The final control system model is shown in Fig. 4c, where $\bar{C}$ has been replaced by (7) and the diagram has been simplified. It is important to note that because the surgical robot is physically separated from the delay, its model does not need to be known as we have access to the surgical robot's position in real time (please note that the only measurement we cannot access in real time is the distance between the surgical robot and the heart). A slight disadvantage of this approach is that while the surgical robot will follow the heart motion on the fly, it will follow the surgeon's hand motions (in the ultrasound images) only after a delay. However, past research has demonstrated that a surgeon is capable of operating when there are delays up to 300 ms in transmission of motion commands to the teleoperated robot [18], thus an image acquisition delay of around 40 ms (25 Hz acquisition rate) is within the acceptable range.

VI. Simulation Results

This proposed controller was simulated in Simulink. The actual heart motion is calculated from a series of ultrasound images and a clinical ECG signal. The average of consecutive heart beats is frequency matched to the heart rate of a recorded ECG from a clinical patient in the MITBIH Database hosted by PhysioNet [19] and is presented in Fig. 5. A time delay of 100 ms and an acquisition rate of 25 Hz is used to simulate the delay and down sampling caused by the

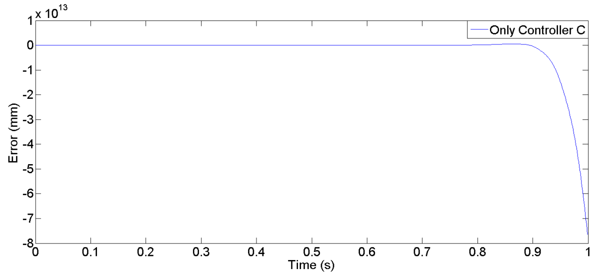

Fig. 6: The distance between the heart wall and the surgical instrument's tip when only a PID controller is used and the delay is present in the system. This case has unacceptable performance as the distance between the surgical tool and the heart wall continually increases.

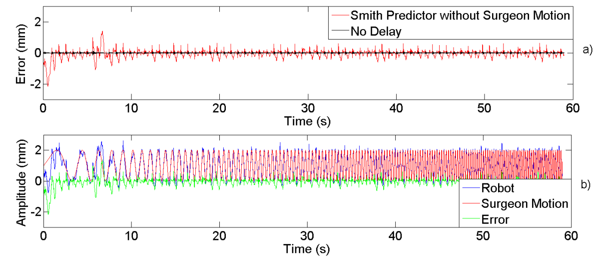

Fig. 7: The distance between the heart wall and the robot end effector when the surgeon's hand motion is removed (a) and when it follows a chirp signal with a frequency ranging between 0.1 Hz and 2 Hz with an amplitude of 2 mm (b).

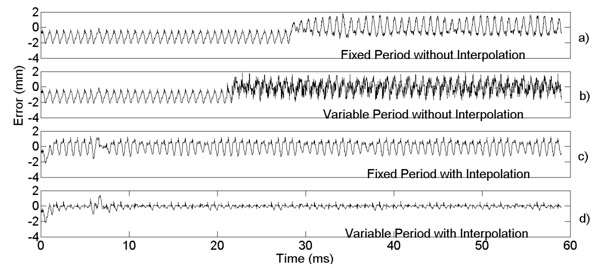

Fig. 8: A comparison of the error when ZOH interpolation a) and b) or cubic interpolation c) and d) or is used and when the estimated heart beat length is updated b) and d) or not updated a) and c).

ultrasound image acquisition and processing. The four gain parameters K_1-K_4 are set to 1, 9, 10, and 9 respectively. The output of this system should follow the surgeon's hand motion. Therefore, the distance between the heart wall and the needle tip should be equal to the surgeon's hand motion. The performance of this system is evaluated by calculating the mean error and the integrated squared error (ISE), which is calculated using (8) where ε is the error value in question.

$$ISE = \sum \varepsilon^2 \tag{8}$$

To begin, the system is simulated without the Smith Predictor or the past heart beat motion compensation. The distance between the heart wall and the surgical tool tip steadily increases as is shown in Fig. 6. To determine the best possible performance, the delay is removed from the system, and hence the Smith Predictor is also removed. The result is shown by the black line in Fig. 7a. The mean error is 0.01 mm and the mean ISE value is $2{\times}10^{-4}$ mm^2. Next, the delay and the Smith Predictor are returned to the system. The surgeon's hand motion is set to zero, the slow data was upsampled using cubic interpolation, and the estimated heart rate is updated by an EKF. The result is shown by the red line in Fig. 7a. The mean error is 0.15 mm and the normalized ISE value is 0.07 mm^2.

Next, a chirp signal with an amplitude of 2 mm and a frequency ranging from 0.1 Hz to 5 Hz is used to represent the surgeon's hand motion. The result is shown in Fig. 7b. The mean error is 0.15 mm and the normalized ISE value is 0.07 mm^2, which is equal to the mean error and mean ISE value of the case when the surgeon's hand motion is removed. This suggests that the surgeon's hand motion does not affect the performance of the predictive control loop.

Finally, the effect of upsampling the slowly sampled data with a cubic interpolator and the effect of updating the length of the estimated past heart beat are studied. The chirp signal described above is included as the surgeon's hand motion in each of the following trials. The performance of each trial is compared based on the error calculated as the distance between the surgical tool's motion and the surgeon's hand motion. Ideally, these two trajectories should be identical. For the first two trials, a zero order hold (ZOH) is used to upsample the estimated heart motion and the distance between the surgical tool and the heart. In the first trial, the length of the past heart beat is set to 803 ms, the average heart beat length, and is kept constant throughout the trial - see Fig. 8a. In the second, the estimated heart rate is updated by an EKF - see Fig. 8b. The actual heart rate of the heart motion signal (see Fig. 5) changes throughout the trial. The mean error and mean ISE values are 0.95 mm and 1.12 mm^2 for the first trial and 0.82 mm and 0.98 mm^2 for the second trial. For the third and fourth trials, cubic interpolation is used to increase the sampling rate of the past heart motion and the distance between the needle and the heart wall. In the third trial the heart rate is not updated - see Fig. 8c; whereas in the fourth it is updated by an EKF - see Fig. 8d. The resulting mean error and mean ISE values are 0.57 mm and 0.42 mm^2 for the third trial and 0.15 mm and 0.07 mm^2 for the fourth trial. The best performance occurs when the estimated heart rate is updated and cubic interpolation is used.

VII. Experimental Results

Following the successful simulation of the system, preliminary experiments are performed with a teleoperated 1 DOF surgical tool under ultrasound guidance. The experimental setup - see Fig. 9 - includes a heart simulator and a 1 DOF motion compensating surgical tool. The motion of each is actuated by a linear voice coil motor with a 20 mm and 12 mm trajectory respectively (NCC20-18-02-1X, H2W Technologies Inc, Valencia CA). The position of the surgical tool and the heart simulator is measured by a linear potentiometer position sensor (A-MAC-B62, Midori America Corp, Fullerton CA) attached to each voice coil. The motion of the entire system is captured by three dimensional ultrasound images acquired from a SONOS 7500 (Phillips Medical, Andover, MA). A more detailed description of the

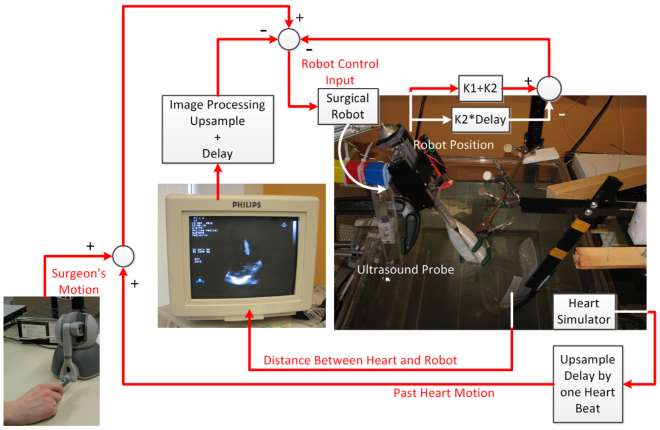

Fig. 9: The experimental setup. A linear voice coil motor actuates a needle which follows the heart simulator based on ultrasound guidance.

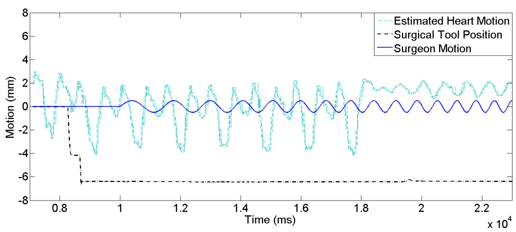

Fig. 10: The motion of the surgical tool tip and the corresponding distance between the simulated heart and the tool tip when no Smith Predictor or estimated heart motion is used.

experimental setup can be found in [15].

The trajectory of the point on the simulated heart directly in front of the surgical tool tip is obtained from ultrasound images and is shown by the light blue line in Figs. 10, 11, and 12. Two trials evaluating the effect of using interpolation are carried out. The total error in each trial is calculated from the ultrasound image and hence, is quite noisy. The estimated heart rate is not updated to reflect the current heart beat length and is set to the average heart rate. A chirp signal with an amplitude of 2 mm centered at zero and a frequency ranging from 0.1 Hz to 5 Hz is added to each trial to represent the surgeon's hand motion. First, the Smith Predictor and estimated heart motion are removed from the system. The result is shown in Fig. 10 and is very poor, as expected. The mean error and mean ISE are 4.31 mm (68% of the heart motion) and 18.59 mm^2 respectively.

Next the Smith Predictor and estimated heart motion are

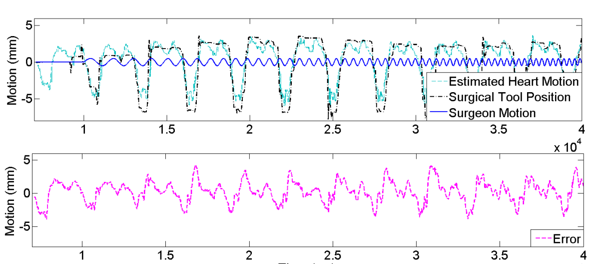

Fig. 11: The motion of the surgical tool tip and the corresponding distance between the simulated heart and the tool tip when cubic interpolation is used.

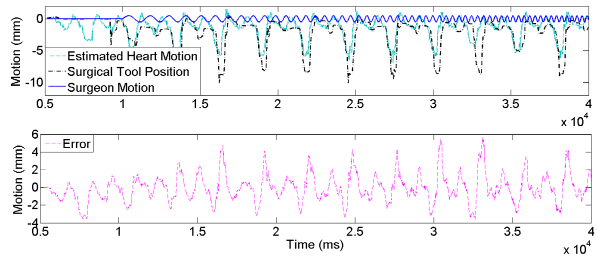

Fig. 12: The motion of the surgical tool tip and the corresponding distance between the simulated heart and the tool tip when ZOH interpolation is used.

TABLE II: A summary of the simulation and experimental errors.

	Absolute Mean Error (mm)	Mean ISE (mm^2)
Simulation Results		
No Smith Predictor or delay no surgeon motion	0.01 (0.48%)	2×10^{-4}
Smith Predictor with delay no surgeon motion	0.15 (7.2%)	0.07
Smith Predictor with delay Chirp surgeon motion	0.15 (7.2%)	0.07
Experimental Results (delay included)		
Experimental with cubic interpolation	1.24 (14%)	1.53
Experimental with ZOH interpolation	1.23 (15%)	1.51
Experimental without Smith Predictor or Past Heart Motion	4.31 (68%)	18.59

returned to the system. The result of the cubic interpolation case is shown in Fig. 11 and the result of the ZOH interpolation case is shown in Fig. 12. The error calculations are done using the section of data where the surgical tool is being actuated. The mean error and mean ISE values are 1.24 mm (14% of the heart motion) and 1.53 mm^2 when cubic interpolation is used and 1.23 mm (15% of the heart motion) and 1.51 mm^2 in the ZOH case. These errors are larger than those reported in the previous section, which is to be expected as the measurements are taken from noisy ultrasound images. However, the use of the Smith Predictor greatly reduces the error as compared to when it is not present.

VIII. Concluding Remarks

This paper proposes a predictive feedback control system for image-guided teleoperated beating-heart surgery. This predictive control system ensures that the distance between the heart wall and the robot's end effector (i.e., surgical instrument) is commanded by the surgeon's hand motions that are input via a user interface. For estimating the heart's motion, typically ultrasound images are used because they are inexpensive to obtain, minimally invasive, and can visualize through blood, which is required for intracardiac surgery. Because the ultrasound images must be acquired and processed, a time delay is introduced into the control system. If this delay is not compensated for, the system may become unstable in the worst case or show unacceptable tracking errors in the mild case.

In this paper, a Smith Predictor is added to the feedback control system to compensate for the above-mentioned delay. In this application, the Integrated Squared Error is greatly reduced in the simulations by incorporating a Smith Predictor into the design. The low sampling rate of the ultrasound and the variable heart beat length are also accounted for.

Future work will focus on improving the prediction of the heart's motion by using past and current measurements to estimate future heart positions.

References

[1] D. T. Kettler, R. D. Plowes, P. M. Novotny, N. V. Vasilyev, P. J. del Nido, and R. D. Howe, "An active motion compensation instrument for beating heart mitral valve surgery," in *IEEE/RSJ International Conference on Intelligent Robots and Systems*, 2007, pp. 1290–1295.

[2] M. J. Mack, "Pro: beating-heart surgery for coronary revascularization:is it the most important development since the introduction of the heart-lung machine?" *Annals of Thoracic Surgery*, vol. 70, no. 5, pp. 1779–1781, 2000.

[3] E. Bogatyrenko, U. D. Hanebeck, and G. Szabo, "Heart surface motion estimation framework for robotic surgery employing meshless methods," in *IEEE/RSJ International Conference on Intelligent Robots and Systems*, 2009, pp. 67–74.

[4] M. F. Newman, J. L. Kirchner, B. Phillips-Bute, V. Gaver, H. Grocott, R. H. Jones, D. B. Mark, J. G. Reves, and J. A. Blumenthal, "Longitudinal assessment of neurocognitive function after coronary-artery bypass surgery," *New England Journal of Medicine*, vol. 344, no. 6, pp. 395–402, 02/08 2001.

[5] S. G. Yuen, D. P. Perrin, N. V. Vasilyev, P. J. del Nido, and R. D. Howe, "Force tracking with feed-forward motion estimation for beating heart surgery," *IEEE Transactions on Robotics*, vol. 26, no. 5, pp. 888–896, 2010.

[6] R. Ginhoux, J. Gangloff, M. de Mathelin, L. Soler, M. M. A. Sanchez, and J. Marescaux, "Active filtering of physiological motion in robotized surgery using predictive control," *IEEE Transactions on Robotics*, vol. 21, no. 1, p. 67, 2005.

[7] S. Yuen, S. Kesner, N. Vasilyev, P. Del Nido, and R. Howe, "3d ultrasound-guided motion compensation system for beating heart mitral valve repair," in *Medical Image Computing and Computer-Assisted Intervention MICCAI 2008*, ser. Lecture Notes in Computer Science. Springer Berlin / Heidelberg, 2008, vol. 5241, pp. 711–719.

[8] S. Chandra, I. S. Salgo, L. Sugeng, L. Weinert, W. Tsang, M. Takeuchi, K. T. Spencer, A. O'Connor, M. Cardinale, S. Settlemier, V. Mor-Avi, and R. M. Lang, "Characterization of degenerative mitral valve disease using morphologic analysis of real-time three-dimensional echocardiographic images / clinical perspective," *Circulation: Cardiovascular Imaging*, vol. 4, no. 1, pp. 24–32, 2011.

[9] S. G. Yuen, P. M. Novotny, and R. D. Howe, "Quasiperiodic predictive filtering for robot-assisted beating heart surgery," in *Robotics and Automation, 2008. ICRA 2008. IEEE International Conference on*, 2008, pp. 3875–3880.

[10] T. J. Franke, O. Bebek, and M. C. Cavusoglu, "Improved prediction of heart motion using an adaptive filter for robot assisted beating heart surgery," in *IEEE/RSJ International Conference on Intelligent Robots and Systems*, 2007, pp. 509–515.

[11] O. Bebek and M. C. Cavusoglu, "Intelligent control algorithms for robotic-assisted beating heart surgery," *IEEE Transactions on Robotics*, vol. 23, no. 3, pp. 468–480, 2007.

[12] R. Ginhoux, J. A. Gangloff, M. F. de Mathelin, L. Soler, J. Leroy, and J. Marescaux, "Model predictive control for tracking of repetitive organ motions during teleoperated laparoscopic interventions," in *European Control Conference*, 2003.

[13] B. D. Hoit, "Pericarditis," September 2006. [Online]. Available: http://www.merckmanuals.com/professional/cardiovascular_disorders/pericarditis/pericarditis.html

[14] M. Osranek, F. Bursi, P. W. OLeary, C. J. Bruce, L. J. Sinak, K. Chandrasekaran, and J. B. Seward, "Hand-carried ultrasound-guided pericardiocentesis and thoracentesis," *Journal of the American Society of Echocardiography*, vol. 16, no. 5, pp. 480–484, 5 2003.

[15] P. M. Novotny, J. A. Stoll, P. E. Dupont, and R. D. Howe, "Real-time visual servoing of a robot using three-dimensional ultrasound," in *IEEE International Conference on Robotics and Automation*, 2007, pp. 2655–2660.

[16] O. J. M. Smith, "Closer control of loops with dead time," *Chemical Engineering Progress*, vol. 53, pp. 217–219, 1957.

[17] M. Cavusoglu, D. Feygin, and F. Tendick, "A critical study of the mechanical and electrical properties of the phantom haptic interface and improvements for high-performance control," *Presence: Teleoperators and Virtual Environments*, no. 6, p. 555, 2002.

[18] R. Rayman, S. Primak, R. Patel, M. Moallem, R. Morady, M. Tavakoli, V. Subotic, N. Galbraith, A. van Wynsberghe, and K. Croome, *Effects of Latency on Telesurgery: An Experimental Study*, ser. Medical Image Computing and Computer-Assisted Intervention. Springer Berlin / Heidelberg, 2005, vol. 3750, pp. 57–64.

[19] A. L. Goldberger, L. A. N. Amaral, L. Glass, J. M. Hausdorff, P. C. Ivanov, R. G. Mark, J. E. Mietus, G. B. Moody, C.-K. Peng, and H. E. Stanley, "PhysioBank, PhysioToolkit, and PhysioNet: Components of a new research resource for complex physiologic signals," *Circulation*, vol. 101, no. 23, pp. e215–e220, 2000 (June 13), circulation Electronic Pages: http://circ.ahajournals.org/cgi/content/full/101/23/e215 PMID:1085218; doi: 10.1161/01.CIR.101.23.e215.